

High-temperature series expansion of the spin correlation functions in B-spinel lattice

This article has been downloaded from IOPscience. Please scroll down to see the full text article.

1998 J. Phys.: Condens. Matter 10 3611

(<http://iopscience.iop.org/0953-8984/10/16/013>)

View [the table of contents for this issue](#), or go to the [journal homepage](#) for more

Download details:

IP Address: 171.66.16.209

The article was downloaded on 14/05/2010 at 13:00

Please note that [terms and conditions apply](#).

High-temperature series expansion of the spin correlation functions in B-spinel lattice

M Hamedoun[†], M Houssa, N Benzakour and A Hourmatallah

Laboratoire de Physique du Solide, Université Sidi Mohammed Ben Abdellah,
Faculté des Sciences Dhar Mahraz, BP 1796, Fes, Morocco

Received 29 July 1997, in final form 3 February 1998

Abstract. High-temperature series expansion of the spin correlation functions on the B-spinel lattice are computed to order 6 in $\beta = 1/k_B T$ for Heisenberg model having both nearest- and next-nearest-neighbour exchange integrals. The results are given for various neighbour correlations (up to the third). The behaviour with the temperature and the site dilution is presented. The obtained results provide a useful tool for a straightforward interpretation and understanding of experimental data. The approach is applied to the experimental results of the B-spinel $\text{ZnCr}_{2x}\text{Al}_{2-2x}\text{S}_4$ in the dilution range $0.85 \leq x \leq 1$. The critical temperature and the critical exponents for the susceptibility and the correlation length are deduced by applying the Padé approximant methods. The following estimates are obtained for the familiar critical exponents: $\nu = 0.691 \pm 0.011$ and $\gamma = 1.382 \pm 0.012$. These values are not sensitive to the dilution ratio x . The transition temperatures as a function of x obtained by the present theory are found to be in excellent agreement with the experimental ones.

1. Introduction

Some previous works, using series expansion methods for the spinel lattice, have restricted themselves to nearest-neighbour coupling and non-random lattice [1] or to the restricted order in β [2]. Nevertheless, there exists a considerable need for more terms in order to study several unresolved problems.

In this work, it is intended to extend the development of the high-temperature series expansion (HTS) of the spin correlation functions to the order 6 in β with nearest-neighbour (n.n.) and next-nearest-neighbour (n.n.n.) interactions, J_1 and J_2 respectively, for the diluted B-spinel lattice $\text{AB}_{2x}\text{B}'_{2-2x}\text{X}_4$. In this latter the magnetic B and the diamagnetic B' ions are located in the tetrahedral sites of the cubic spinel lattice. The A ions are divalent metal ions. The X ions can be anions of the chalcogenide group.

To deduce the spin correlation function: $\gamma_{ij} = \langle \mathbf{S}_i \cdot \mathbf{S}_j \rangle / S(S+1)$ between spins at site i and j , we have used the diagrammatic representation performed by Stanley and Kaplan (SK) [3, 4]. Their method is general and can be applied to any lattice. This semiclassical treatment is a simplification of the more complex procedure of Rushbrooke and Wood [5] used for the calculation of the susceptibility in the quantum-mechanical case. In order to obtain more information about the magnetic properties in the B-spinel system, we have calculated the spin correlation functions between first, second and third n.n. spins γ_1, γ_2

[†] Corresponding author.

and γ_3 respectively. To study the critical region of the particular case of the B-spinel lattice $\text{ZnCr}_{2x}\text{Al}_{2-2x}\text{S}_4$ in the long-range ordering $0.85 \leq x \leq 1$ [6], we have applied the Padé approximant (PA) methods to the HTS of the spin correlation function, the magnetic susceptibility $\chi(\mathbf{k})$ and the correlation length $\xi(T)$. The critical temperature T_N , the critical exponents γ for the magnetic susceptibility and ν for the correlation length are deduced. In the whole range of concentration $0.85 \leq x \leq 1$, the exponents γ and ν are found to be equal to 1.382 ± 0.012 and 0.691 ± 0.011 respectively.

It is known that the measurement of the neutron scattering is a powerful tool for the investigation of the spin correlation. Neutron scattering experiments in $\text{ZnCr}_{2x}\text{Al}_{2-2x}\text{S}_4$ with $0.85 \leq x \leq 1$ were carried out with the 800-cell multidetector diffractometer installed at the Siloé reactor of the CEN Grenoble and on the D1A diffractometer of the Laue–Langevin institute. More details on the experimental conditions are given elsewhere in [7]. The magnetic diffuse peaks are studied by the Ornstein–Zernike form with a Lorentzian line. The experimental thermal variations of the correlation length are obtained for $x = 1, 0.90$ and 0.85 . A qualitative analysis of this variation shows that the critical exponent ν must be the same for the three concentrations. Experimental values of T_N/J_1 deduced from the neutron diffraction measurements are in good agreement with those obtained by HTS extrapolated with the PA methods.

2. Theory and results

Starting with the zero-field Heisenberg Hamiltonian

$$H = -2 \sum_{i,j} J_{ij} \mathbf{S}_i \cdot \mathbf{S}_j \quad (1)$$

where the summation run over all pairs of n.n. and n.n.n. interactions J_1 and J_2 respectively. The expansion of the spin correlation function in powers of β is obtained as follows [3]

$$\langle \mathbf{S}_i \cdot \mathbf{S}_j \rangle = \frac{\text{Tr} \mathbf{S}_i \cdot \mathbf{S}_j e^{-\beta H}}{\text{Tr} e^{-\beta H}} = \sum_{l=0} \frac{(-1)^l}{l!} \alpha_l \beta^l \quad (2)$$

with

$$\alpha_l = \nu_l - \sum_{k=0}^{l-1} C_k^l \alpha_k \mu_{l-k} \quad \nu_m = \langle \mathbf{S}_i \cdot \mathbf{S}_j H^m \rangle_{\beta=0} \quad (3)$$

and $\mu_m = \langle H^m \rangle_{\beta=0}$.

This leads to a diagrammatic representation given in [4]. The calculation of the coefficients of the γ_i according to the diagrammatic method involves two separate phases.

(a) The finding and cataloguing of all the diagrams or graphs which can be constructed from one dashed line connecting the sites 0 and i and l straight lines, and the determination of diagrams whose contribution is nonvanishing.

(b) Counting the number of times that a diagram can occur in the spinel lattice. Step (a) has already been accomplished in the SK work. Step (b), however, is very tedious. In our case, we have to deal with the two Heisenberg constant couplings: J_1 and J_2 between first and second n.n. in the spinel system: AB_2X_4 (with only BB interactions).

For each topological form of a given diagram, a full line can either represent J_1 or J_2 . We must, thus, derive from each topological form a class of diagrams; each of them represents a term of the series as: $J_1^m J_2^n$ ($m, n = 0, 1, \dots, l$ and $m + n = l$) for the l th order. This is especially the limiting factor in how far one can carry the expansion.

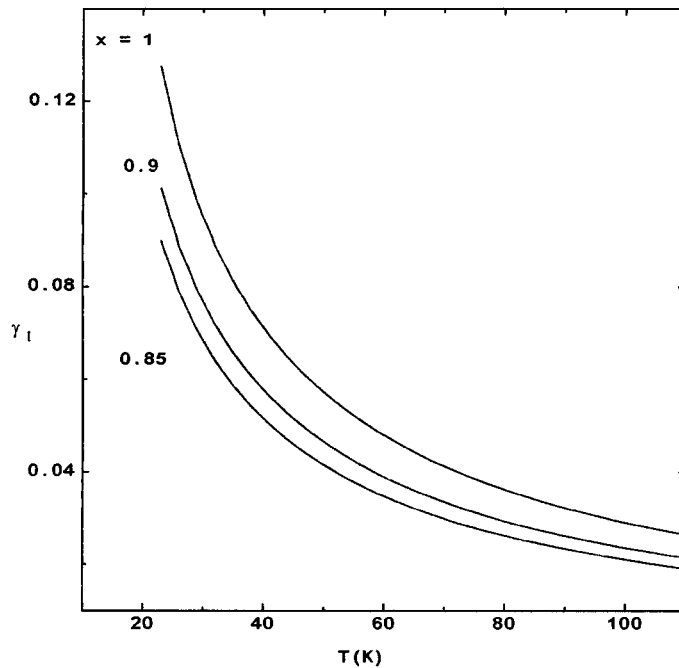


Figure 1. The first-n.n. spin correlation function γ_1 plotted against the temperature for the system $\text{ZnCr}_{2x}\text{Al}_{2-2x}\text{S}_4$ for $x = 1, 0.9$ and 0.85 .

In this fashion, we calculated all of the coefficients required for the calculation of the spin correlation functions γ_i ($i = 1-3$) in the case of a diluted B-spinel lattice $\text{AB}_{2x}\text{B}'_{2-2x}\text{X}_4$ through order $l = 6$, and the results of this calculation are given in appendix A. In the γ_i with $i \geq 4$ the series contain, only, terms in β^l with $l \geq 4$.

Equation (2) combined with the expressions of appendix A and the results of appendix B permits the computation of the spin correlation functions γ_i ($i = 1-3$) in terms of powers of β , x and mixed powers of J_1 and J_2 .

For a given set of the J_i of a diluted B-spinel system $\text{AB}_{2x}\text{B}'_{2-2x}\text{X}_4$ with $S = \frac{3}{2}$ (in which we shall be interested here) we can derive the spin correlation function and its dependence upon disorder (variation with temperature T and magnetic site dilution x). We have adopted a rigid model for the constant couplings, where the latter are not very sensitive to the temperature and the magnetic disorder variation. We will especially consider the helimagnetic spinel $\text{ZnCr}_{2x}\text{Al}_{2-2x}\text{S}_4$ in the long-range order (LRO) region $0.85 \leq x \leq 1$. The values of J_1 and J_2 used are 2.2 K and 1.1 K respectively. They are obtained on the basis of neutron and magnetic results combined with the mean-field theory [8].

Figures 1-3 show the evolution of the first-, second- and third-n.n. spin correlation functions with temperature for $x = 1, 0.9$ and 0.85 in diluted ZnCr_2S_4 system (e.g. $\text{ZnCr}_{2x}\text{Al}_{2-2x}\text{S}_4$). The main feature of these curves is the decrease with T and x , i.e. the order is destroyed by the thermal disorder and the magnetic dilution. For the pure compound and for all temperatures, the γ_1 is positive, the γ_2 is negative and the γ_3 is positive. This sequence $+ - +$ is a characteristic of a non-linear ordering. From figure 3 we see that γ_3 is negative at very low temperature and for diluted samples. When the disorder is augmented it becomes positive.

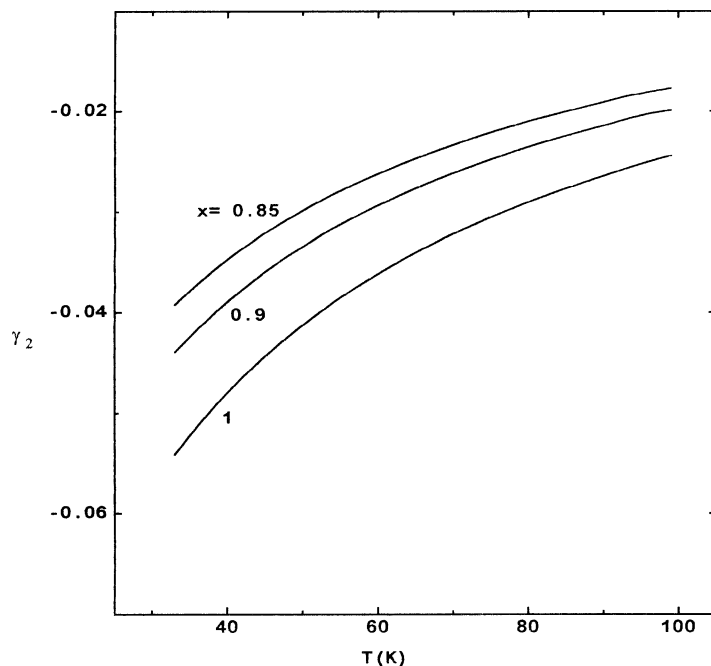


Figure 2. The second-n.n. spin correlation function γ_2 versus temperature for $\text{ZnCr}_{2x}\text{Al}_{2-2x}\text{S}_4$ for the same concentrations.

Since we are interested in estimating critical points we have used the PA methods to study the dependence of the critical temperature T_N on the relative strength of J_1 , J_2 and the ratio of dilution x . The T_N is estimated as the temperature at which the γ_1 diverges [7]. Using [3, 4] PA we have calculated the ratio T_N/J_1 in the LRO region of the system $\text{ZnCr}_{2x}\text{Al}_{2-2x}\text{S}_4$. Figure 4 shows the obtained T_N/J_1 (solid line) against dilution x . In this figure we have included, for comparison, the experimental results obtained by neutron diffraction given in [6]. One can see the excellent agreement between the theoretical and experimental results.

The wavelength-dependent susceptibility $\chi(\mathbf{k})$ and correlation function $S(\mathbf{k})$ are defined as

$$\chi(\mathbf{k}) = g\mu_B^2\beta \sum_{i,j} \langle \mathbf{S}_i \cdot \mathbf{S}_j \rangle e^{-i\mathbf{k} \cdot \mathbf{R}_{ij}} \quad (4)$$

and

$$S(\mathbf{k}) = \sum_{i,j} \langle \mathbf{S}_i \cdot \mathbf{S}_j \rangle e^{-i\mathbf{k} \cdot \mathbf{R}_{ij}} \quad (5)$$

where μ_B is the Bohr magneton, g the gyromagnetic ratio and \mathbf{R}_{ij} is the separation between the spins i and j .

In order to obtain a qualitative measure of the correlation length $\xi(T)$ for a given temperature T , we expand the correlation function $S(\mathbf{k})$ in a Taylor expansion about the magnetic reciprocal lattice \mathbf{Q} of the given system [11]:

$$S(\mathbf{k}) = S(\mathbf{Q})[1 - \xi^2(T)(\mathbf{k} - \mathbf{Q})^2 + o(\mathbf{k} - \mathbf{Q})^4]. \quad (6)$$

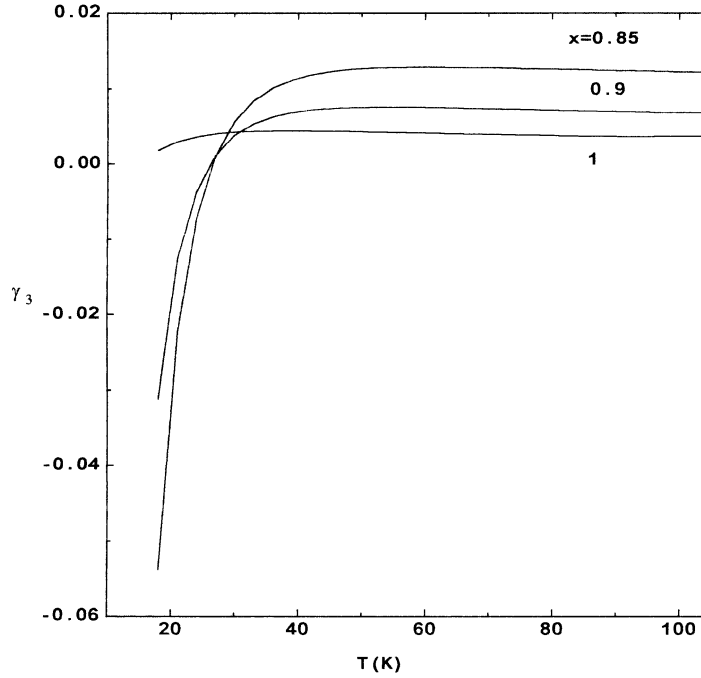


Figure 3. The same as figure 2 for the third-n.n. spin correlation function γ_3 .

Recasting this in the Ornstein–Zernike form, the following asymptotic form is obtained:

$$S(\mathbf{k}) = \frac{S(\mathbf{Q}) \cdot \kappa^2(T)}{[\kappa^2(T) + (\mathbf{k} - \mathbf{Q})^2]} \quad (7)$$

where $\kappa(T) = \xi^{-1}(T)$.

In the B-spinel lattice and for the particular case of the helimagnetic structure with wave-vector $\mathbf{Q} = [0, 0, k]$, we obtain

$$S(\mathbf{k}) = 4 \left[1 + \gamma_{aa} + \gamma_{ab} \cos\left(\frac{\pi k}{2}\right) + \gamma_{ac} \cos(\pi k) \right]. \quad (8)$$

$\gamma_{aa} = 2\gamma_1 + 4\gamma_3$ is the in-plane correlation. $\gamma_{ab} = 4\gamma_1 + 8\gamma_2$ is the correlation between neighbouring planes. $\gamma_{ac} = 4\gamma_2 + 8\gamma_3$ is the correlation between the second-neighbour planes.

Above T_N , short-range order is present and gives rise to diffuse scattering contribution strongly peaked at the \mathbf{Q} -value associated with the helical order [6, 7]. The maximization of $S(\mathbf{k})$ with respect to $k = k_0$ gives

$$\cos\left(\frac{\pi k_0}{2}\right) = -\frac{1}{4} \frac{\gamma_{ab}}{\gamma_{ac}}. \quad (9)$$

k_0 is related to the helix angle θ by $\theta = \pi k_0/2$

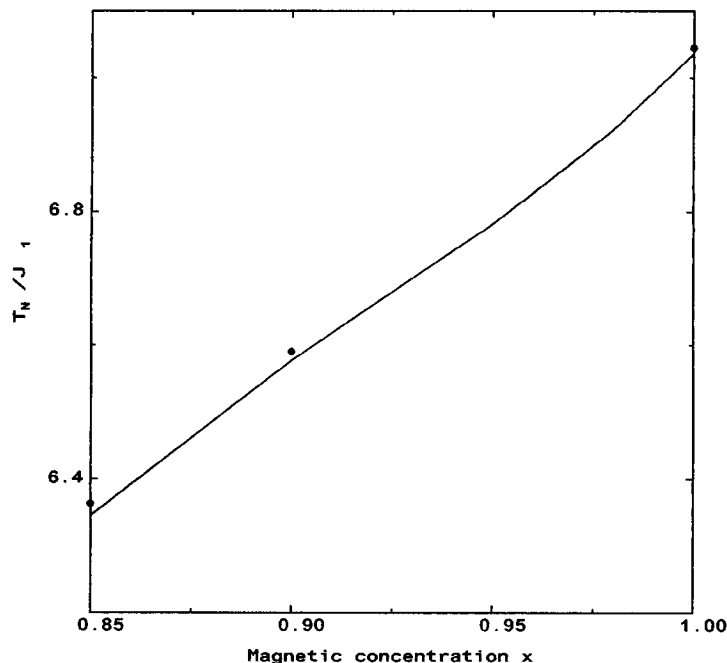


Figure 4. Variation of the T_N/J_1 with the magnetic concentration x in $\text{ZnCr}_{2x}\text{Al}_{2-2x}\text{S}_4$ for $0.85 \leq x \leq 1$. The circles are the experimental points reported in [6]. The line is the result obtained from the high-temperature series expansion extrapolated with the Padé approximant methods.

Expanding the cosines of equation (8) in the Taylor expansion about $k = k_0$ and using the equation (6) we obtain

$$\left(\frac{\xi}{a}\right)^2 = \frac{1}{8S(k_0)} \left[-\gamma_{ac} + \frac{\gamma_{ab}^2}{16\gamma_{ac}} \right] \quad (10)$$

where a is the lattice parameter.

The simplest assumption that one can make concerning the nature of the singularity of the magnetic susceptibility $\chi(\mathbf{k})$ and the correlation length $\xi(T)$ is that in the neighbourhood of the critical points the above two functions exhibit an asymptotic behaviour.

$$\chi(\mathbf{k}) \propto (T_N - T)^{-\gamma} \quad (11)$$

and

$$\xi^2(T) \propto (T_N - T)^{-2\nu}. \quad (12)$$

T_N represents the critical temperature, deduced by the PA methods, γ and ν the critical exponents.

Representation of the series expansions of $\chi(\mathbf{k})$ and $\xi^2(T)$ by [3, 4] AP would enable us to find γ and 2ν . By finding $\lim_{y \rightarrow y_N} (y - y_N)(d/dy) \log(F(y))$ ($F(y) = \chi, \xi^2$) with $y = J_1/T$ and $y_N = J_1/T_N$ we have obtained the values of the above two critical exponents in the case of the B-spinel $\text{ZnCr}_{2x}\text{Al}_{2-2x}\text{S}_4$.

Using the helix angle θ deduced from the position of the magnetic satellite of the neutron diffraction pattern [8], $\theta(x = 1) = 71^\circ$, $\theta(x = 0.90) = 68^\circ$ and $\theta(x = 0.85) = 64^\circ$, we have obtained the central values of γ and ν for the three concentrations $\gamma = 1.382 \pm 0.012$

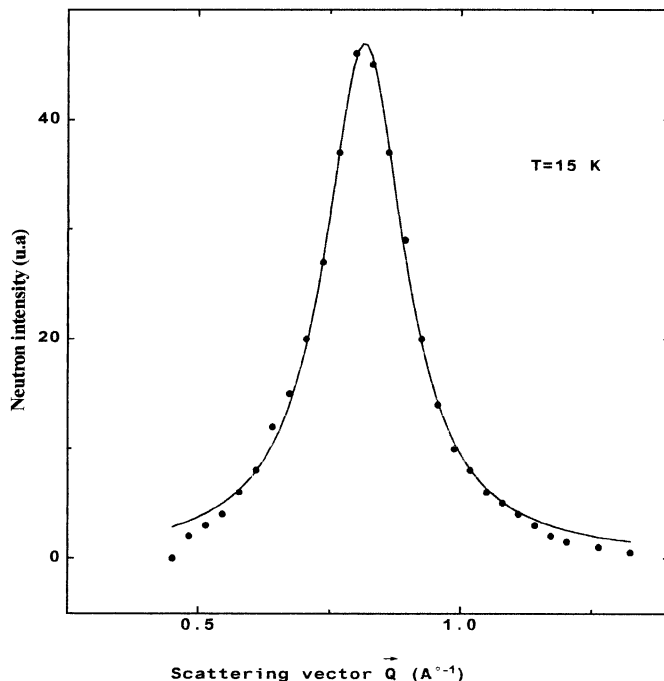


Figure 5. The critical neutron scattering observed in $\text{ZnCr}_{2x}\text{Al}_{2-2x}\text{S}_4$ for $x = 0.9$ and at $T = 15$ K. The solid line represents the fit to the Lorentzian form of (8) (see text). The circles are the experimental points.

and $\nu = 0.691 \pm 0.011$. These values may be compared with those of the 3D Heisenberg model, namely, 1.3866 ± 0.0012 and 0.7054 ± 0.0011 [9, 10]. The agreement is excellent.

In order to study the thermal variation of $\xi(T)$, we have analysed the magnetic diffuse intensity by the Lorentzian form of (7). Figure 5 shows an example of this fit in the case of the compound $x = 0.9$ and at $T = 15$ K. For all studied temperatures and dilutions the fits are excellent. The thermal variations of $\xi(T)$ for $x = 1, 0.9$ and 0.85 are presented in figure 6. The results show an unexpected feature: the onset of long-range order at T_N is not associated with a maximum in $\xi(T)$. Indeed $\xi(T)$ increases on further cooling. There is possibly a break in the slope of the curve of $\xi(T)$ against temperature at T_N . A similar behaviour is observed in the system $\text{KMn}_c\text{Zn}_{1-c}\text{F}_3$ near the percolation threshold [12]. An explanation based on the cluster topology of spins in the backbone of the infinite cluster is proposed [12].

The curvatures of $\xi(T)$ around T_N of each dilution are identical, hence the value of the critical exponent ν is almost the same for the three concentrations.

3. Conclusion

The first three spin correlation functions for the diluted B-spinel lattice $\text{AB}_{2x}\text{B}'_{2-2x}\text{X}_4$ were determined with the nearest- and next-nearest-neighbour interactions to order 6 in β by the high-temperature series expansion. We applied the results to the particular experimental B-spinel $\text{ZnCr}_{2x}\text{Al}_{2-2x}\text{S}_4$ in the long-range order region $0.85 \leq x \leq 1$. The spin correlations persist up to about 100 K. The sequence sign of the γ_1, γ_2 and γ_3 for $T > T_N$ is compatible

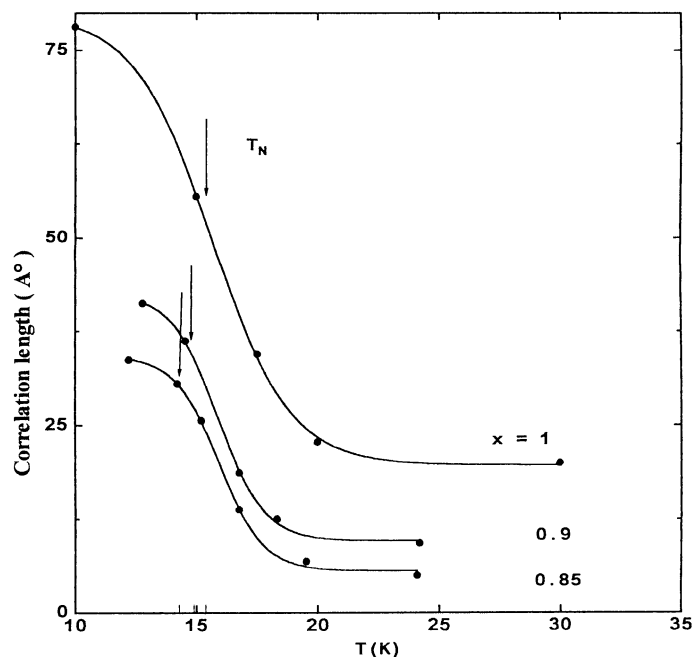


Figure 6. Correlation length versus temperature in $\text{ZnCr}_{2x}\text{Al}_{2-2x}\text{S}_4$ for $x = 1, 0.9$ and 0.85 as derived from scans such as that shown in figure 5. The arrows indicate the critical temperature T_N . Lines are guides for the eye.

with a non-linear order. The short-range ordering for T above T_N is characterized by a helical spin arrangement similar to that observed in the ordered state for T below T_N .

High-temperature series expansion extrapolated with Padé approximants is shown to be a convenient method to provide valid estimations of critical temperatures for real magnetic systems [13]. By applying this method to the γ_1 we are estimated the critical temperatures against the dilution x in the long-range order region of $\text{ZnCr}_{2x}\text{Al}_{2-2x}\text{S}_4$. The obtained results are in good agreement with those obtained by experimental neutron diffraction. The critical exponents of the magnetic susceptibility γ and the correlation length ν are found equals to 1.382 ± 0.012 and 0.691 ± 0.011 in the whole range of concentration $0.85 \leq x \leq 1$. These values are compatible with those of 3D Heisenberg model. A qualitative study of the experimental thermal variation of the correlation length shows the independence of the critical exponent ν with the dilution.

According to the Harris criterion [14], since ZnCr_2S_4 is a good 3D Heisenberg system, the critical exponent α of the specific heat is less than zero [9]; hence, the critical exponents are unaffected by dilution.

Similar studies for the short-range order region of $\text{ZnCr}_{2x}\text{Al}_{2-2x}\text{S}_4$ ($x < 0.85$) are under consideration.

Appendix A

The topological diagram type as in SK notation (τ) and the corresponding α_l which are needed to extend the high-temperature series to order $l = 6$ in the case of a B-spinel lattice with n.n. and n.n.n. interactions.

(1)

$$(\tau_1 : \text{---}) [\alpha_1] = \frac{1}{3}$$

$$\alpha_1 = [\alpha_1] x^2 (-2S(S+1)) n^{(i)} J_i$$

(2)

$$\left(\tau_2 : \triangle \right) [\alpha_2] = \frac{2}{9}$$

$$\alpha_2 = [\alpha_2] x^3 (-2S(S+1))^2 \sum_{p,q} n^{(p,q)} J_p J_q$$

(3)

$$\left(\tau_3^1 : \text{---} \right) [\alpha_3]_1 = -\frac{2}{15} \quad \left(\tau_3^2 : \square \right) [\alpha_3]_2 = \frac{2}{9}$$

$$\alpha_3 = (-2S(S+1))^3 \left\{ [\alpha_3]_1 x^2 n^{(i)} J_i^3 + [\alpha_3]_2 x^4 \sum_{p,q,r} n^{(p,q,r)} J_p J_q J_r \right\}$$

(4)

$$\left(\tau_4^1 : \triangle \right) [\alpha_4]_1 = -\frac{8}{45} \quad \left(\tau_4^2 : \triangle \right) [\alpha_4]_2 = -\frac{8}{15}$$

$$\left(\tau_4^3 : \text{---} \right) [\alpha_4]_3 = \frac{8}{27}$$

$$\alpha_4 = (-2S(S+1))^4 \left\{ x^3 \sum_{p,q} n^{(p,q)} ([\alpha_4]_1 J_p^3 J_q + [\alpha_4]_2 J_i^2 J_p J_q) \right. \\ \left. + x^5 \sum_{p,q,r,s} n^{(p,q,r,s)} [\alpha_4]_3 J_p J_q J_r J_s \right\}$$

(5)

$$\left(\tau_5^1 : \text{---} \right) [\alpha_5]_1 = \frac{40}{81} \quad \left(\tau_5^2 : \square \right) [\alpha_5]_2 = -\frac{8}{9}$$

$$\left(\tau_5^3 : \square \right) [\alpha_5]_3 = -\frac{8}{27}$$

$$\left(\tau_5^4 : \square \right) [\alpha_5]_4 = -\frac{8}{27} \quad \left(\tau_5^5 : \text{---} \right) [\alpha_5]_5 = \frac{16}{63}$$

$$\left(\tau_5^6 : \square \right) [\alpha_5]_6 = -\frac{16}{9} \quad \left(\tau_5^7 : \square \right) [\alpha_5]_7 = -\frac{8}{9}$$

$$\left(\tau_5^8 : \triangle \right) [\alpha_5]_8 = -\frac{152}{135}$$

$$\alpha_5 = (-2S(S+1))^5 \left\{ x^2 [\alpha_5]_5 n^i J_i^5 + x^3 \sum_{p,q} [\alpha_5]_8 n^{(p,q)} J_i J_p^2 J_q^2 \right. \\ \left. + x^4 \left(\sum_{p,q,r} ([\alpha_5]_2 n^{(p,q,r)} J_i^2 J_p J_q J_r + [\alpha_5]_3 n^{(p,q,r)} J_p^3 J_q J_r) \right) \right. \\ \left. + [\alpha_5]_4 n^{(p,q,r)} J_p J_q^3 J_r \right\} \quad (\text{A1})$$

$$\begin{aligned}
 & + \sum_{p,q,r,s} [\alpha_5]_6 n^{(p,q,r,s)} J_i J_p J_q J_r J_s + \sum_{p,q,r,s} [\alpha_5]_7 n^{(p,q,r,s)} J_p J_q J_r J_s^2 \\
 & + x^6 [\alpha_5]_1 \sum_{p,q,r,s,h} n^{(p,q,r,s,h)} J_p J_q J_r J_s J_h \}
 \end{aligned}$$

(6)

$$\begin{aligned}
 \left(\tau_6^1 : \begin{array}{c} \diagup \\ \square \\ \diagdown \end{array} \right) [\alpha_6]_1 &= \frac{80}{81} & \left(\tau_6^2 : \begin{array}{c} \diagup \\ \square \\ \diagdown \\ \hline \hline \hline \end{array} \right) [\alpha_6]_2 &= -\frac{16}{27} \\
 \left(\tau_6^3 : \begin{array}{c} \diagup \\ \square \\ \diagdown \\ \hline \hline \hline \end{array} \right) [\alpha_6]_3 &= -\frac{16}{27} & \left(\tau_6^4 : \begin{array}{c} \triangleleft \\ \square \\ \triangleright \end{array} \right) [\alpha_6]_4 &= -\frac{16}{9} \\
 \left(\tau_6^5 : \begin{array}{c} \diagup \\ \square \\ \diagdown \\ \hline \hline \hline \end{array} \right) [\alpha_6]_5 &= -\frac{32}{9} & \left(\tau_6^6 : \begin{array}{c} \square \\ \hline \hline \hline \end{array} \right) [\alpha_6]_6 &= -\frac{304}{135} \\
 \left(\tau_6^7 : \begin{array}{c} \diagup \\ \square \\ \diagdown \\ \hline \hline \hline \end{array} \right) [\alpha_6]_7 &= \frac{16}{45} & \left(\tau_6^8 : \begin{array}{c} \triangle \\ \hline \hline \hline \end{array} \right) [\alpha_6]_8 &= \frac{32}{63} \\
 \left(\tau_6^9 : \begin{array}{c} \diagup \\ \square \\ \diagdown \\ \hline \hline \hline \end{array} \right) [\alpha_6]_9 &= -\frac{16}{9} & \left(\tau_6^{10} : \begin{array}{c} \triangleleft \\ \square \\ \triangleright \end{array} \right) [\alpha_6]_{10} &= -\frac{32}{9} \\
 \left(\tau_6^{11} : \begin{array}{c} \triangleleft \\ \square \\ \triangleright \end{array} \right) [\alpha_6]_{11} &= -\frac{16}{9} & \left(\tau_6^{12} : \begin{array}{c} \triangleleft \\ \square \\ \triangleright \end{array} \right) [\alpha_6]_{12} &= -\frac{16}{9} \\
 \left(\tau_6^{13} : \begin{array}{c} \triangleleft \\ \square \\ \triangleright \end{array} \right) [\alpha_6]_{13} &= -\frac{32}{9} & \left(\tau_6^{14} : \begin{array}{c} \square \\ \hline \hline \hline \end{array} \right) [\alpha_6]_{14} &= -\frac{608}{135} \\
 \left(\tau_6^{15} : \begin{array}{c} \square \\ \hline \hline \hline \end{array} \right) [\alpha_6]_{15} &= -\frac{304}{135} & \left(\tau_6^{16} : \begin{array}{c} \triangle \\ \hline \hline \hline \end{array} \right) [\alpha_6]_{16} &= \frac{16}{15} \\
 \left(\tau_6^{17} : \begin{array}{c} \triangle \\ \hline \hline \hline \end{array} \right) [\alpha_6]_{17} &= \frac{160}{63}
 \end{aligned}$$

$$\begin{aligned}
 \alpha_6 &= (-S(S+1))^6 \left\{ x^3 \left(\sum_{p,q} n^{(p,q)} ([\alpha_6]_7 J_p^3 J_q^3 + [\alpha_6]_8 J_p^5 J_q + [\alpha_6]_{16} J_i^2 J_p^3 J_q \right. \right. \\
 & \left. \left. + [\alpha_6]_{17} J_i^4 J_p J_q \right) \right. \\
 & + x^4 \left(\sum_{p,q,r,s} [\alpha_6]_6 n^{(p,q,r,s)} J_p^2 J_q^2 J_r J_s \right. \\
 & \left. + \sum_{p,q,r,s} n^{(p,q,r,s)} ([\alpha_6]_{14} J_i J_p^2 J_q J_r J_s + [\alpha_6]_{15} J_p^2 J_q^2 J_r J_s) \right) \\
 & + x^5 \left(\sum_{p,q,r,s} n^{(p,q,r,s)} ([\alpha_6]_2 J_p^3 J_q J_r J_s + [\alpha_6]_3 J_p J_q^3 J_r J_s + [\alpha_6]_9 J_i^2 J_p J_q J_r J_s) \right. \\
 & \left. + \sum_{p,q,r,s,h} [\alpha_6]_4 J_p J_q J_r J_s J_h^2 + \sum_{p,q,r,s,h,m} [\alpha_6]_5 n^{(p,q,r,s,h,m)} J_p J_q J_r J_s J_h J_m \right. \\
 & \left. + \sum_{p,q,r,s,h,m} n^{(p,q,r,s,h,m)} [\alpha_6]_{13} J_p J_q J_r J_s J_h J_m \right)
 \end{aligned}$$

$$\begin{aligned}
& + \sum_{p,q,r,s,h} [\alpha_6]_{10} n^{(p,q,r,s,h)} J_i J_p J_q J_r J_s J_h + [\alpha_6]_{11} n^{(p,q,r,s,h)} J_p^2 J_q J_r J_s J_h \\
& + \sum_{p,q,r,s,h} [\alpha_6]_{12} n^{(p,q,r,s,h)} J_p J_q^2 J_r J_s J_h \Big) \\
& + x^7 \sum_{p,q,r,s,h,m} n^{(p,q,r,s,h,m)} [\alpha_6]_{11} J_p J_q J_r J_s J_h J_m \Big\}.
\end{aligned}$$

Our main task is to compute the $n^{(p,q,\dots)}$. The results are given in appendix B for each i th neighbour.

Appendix B

As the $n^{(p,q,\dots)}$ are coefficients of $J_p J_q \dots$, and the latter product is invariant under a change in the order of p, q, \dots , we can sum up the $n^{(p,q,\dots)}$ over all combinations of the (p, q, \dots) . We note $(p, q, \dots) = \sum_{C(p,q,\dots)} n^{(p,q,\dots)}$.

For instance, we note $(122) = n^{(1,2,2)} + n^{(2,1,2)} + n^{(2,2,1)}$ and so on. The (p, q, \dots) are listed in table B1 with their numbers of occurrences in the spinel lattice for each neighbour up to order $l = 6$, and which are necessary for the computation of the γ_i . The dashed lines in the diagrams can either represent a simple straight line as in diagram τ_2 in formulas (A1) or a double straight line as in diagram τ_4^1 or τ_4^2 . This is because the number of occurrences of a diagram in the lattice does not depend on the type of the link between sites but only on the number of sites in the diagram. From these diagrams, only those in expressions (A1) are used.

Table B1.

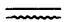







Order l	Diagram type	First n.n.	Second n.n.	Third n.n.
1	(1)	1	0	0
		0	1	0
2	(11)	2	1	1
	(12)	4	2	4
	(22)	2	2	0
3	(111)	2	4	12
	(112)	24	16	40
	(122)	34	27	44
	(222)	18	5	16
	(1111)	0	10	8
4	(1112)	78	85	54
	(1122)	260	217	173
	(1222)	286	202	140
	(2222)	95	60	64
	(11111)	2	18	16
	(11112)	164	289	262
5	(11122)	1010	1002	976
	(11222)	1776	1331	1125
	(12222)	1262	699	294
	(22222)	267	147	95
	(1111)	2	0	0
	(1112)	16	4	2
	(1122)	20	4	4
	(1222)	16	4	6
	(2222)	2	0	0

Table B1. (Continued)

	(11111)	2	2	2
5	(11112)	12	6	4
	(11122)	10	4	2
	(11222)	8	2	8
	(12222)	4	3	2
	(22222)	2	0	0
	(111111)	22	52	58
	(111112)	507	865	1164
6	(111122)	4031	4464	2654
	(111222)	9554	9321	7324
	(112222)	13 413	9669	8485
	(122222)	6634	3262	2684
	(222222)	1253	681	542
	(111111)	0	0	0
6	(111112)	24	0	6
	(111122)	84	6	8
	(111222)	120	12	4
	(112222)	84	6	2
	(122222)	24	0	2
	(222222)	0	0	0
	(111111)	0	0	0
	(111112)	40	14	6
6	(11122)	132	46	22
	(11222)	168	50	34
	(12222)	102	22	18
	(22222)	24	3	2
	(111111)	0	2	4
	(111112)	20	14	16
6	(111222)	56	32	24
	(111222)	64	34	28
	(112222)	44	14	6
	(122222)	8	0	2
	(222222)	0	0	4
	(111111)	0	2	0
	(111112)	36	16	22
6	(111222)	58	33	21
	(111222)	72	33	25
	(112222)	80	22	17
	(122222)	32	17	31
	(222222)	4	2	4
	(111111)	2	8	4
	(111112)	32	38	22
6	(111222)	76	66	56
	(111222)	84	65	51
	(112222)	74	44	32
	(122222)	48	19	14
	(222222)	14	3	2

References

- [1] Jasnow D and Moore M A 1968 *Phys. Rev.* **176** 751
- [2] Rachadi A, Hamedoun M and El Allam D 1996 *Physica B* **222** 160
- [3] Stanley H E and Kaplan T A 1966 *Phys. Rev. Lett.* **16** 981

- [4] Stanley H E and Kaplan T A 1967 *Phys. Rev.* **158** 537
- [5] Rushbrooke G S and Wood P J 1958 *Mol. Phys.* **1** 257
- [6] Hamedoun M, Wiedenmann A, Dormann J L, Nogues M and Rossat-Mignod J 1986 *J. Phys. C: Solid State Phys.* **19** 1781
- [7] Wiedenmann A, Hamedoun M and Rossat-Mignod J 1985 *J. Phys. C: Solid State Phys.* **18** 2549
- [8] Hamedoun M, Rachadi A, Hourmatallah A, El Allam D and Benyoussef A 1995 *Phys. Status Solidi b* **191** 503
- [9] For a review, see Collins M F 1989 *Magnetic Critical Scattering* (Oxford: Oxford University Press)
- [10] Le Guillou J C and Zinn-Justin J 1977 *Phys. Rev. Lett.* **2** 95
- [11] Kawasaki K and Tahir-khel R A 1977 *Phys. Rev. B* **5** 2741
- [12] Cowley R A, Shirane G, Birgeneau B J, Svensson E C and Guggenheim H J 1980 *Phys. Rev. B* **9** 4412
- [13] Moron M C 1996 *J. Phys.: Condens. Matter* **8** 11 141
- [14] Harris A B 1974 *J. Phys. C: Solid State Phys.* **7** 1671